The structural inhomogeneity of lead–cadmium fluoride systems and its implications

2009 J. Phys.: Condens. Matter 21 335107

(http://iopscience.iop.org/0953-8984/21/33/335107)

J. Phys.: Condens. Matter **21** (2009) 335107 (9pp) doi:10.1088/0953-8984/21/33/335107

The structural inhomogeneity of lead–cadmium fluoride systems and its implications

Adalberto Picinin[1,4], **Mauricio A P Silva**[2] **and José Pedro Rino**[3]

[1] FACIP, Universidade Federal de Uberlândia, Avenida João José Dib, 2545, 38302-000, Ituiutaba, MG, Brazil
[2] Departamento de Química, Universidade Federal de Juiz de Fora, Campus Universitário Martelos, 36036-330, Juiz de Fora, MG, Brazil
[3] Departamento de Física, Universidade Federal de São Carlos, Via Washington Luiz, Km 235, 13565-905, São Carlos, SP, Brazil

E-mail: picinin@df.ufscar.br

Received 5 May 2009, in final form 14 July 2009
Published 28 July 2009
Online at stacks.iop.org/JPhysCM/21/335107

Abstract

In this paper we present a detailed study of structural and dynamical properties of the CdF_2–PbF_2 systems. Particular attention is devoted to the processes involving the phase separation, a phenomenon of fundamental importance in the correct description of some dynamical properties, as introduced in our previous works. We show here, that the phase separation trend is observed in the undercooled melt, whether by cooling the liquid below its melting point, or by heating a homogeneous glass at temperatures above T_g. The degree of phase separation depends on the procedure employed to obtain the crystalline materials, and the simplest way to determine this property is by performing an isothermal treatment in the undercooled melt region. The local fluorine environments $Q^{(n)}$, corresponding to fluorine surrounded by nPb and 4-nCd neighbors, is used as a probe in the average local composition. We demonstrate that the increase in the structural inhomogeneity around the composition with $x = 0.35$ is the factor which leads to a better fluorine conducting property for the $Cd_{0.35}Pb_{0.65}F_2$ solid solution, in addition to providing a correct determination of the melting temperature of the $Cd_xPb_{1-x}F_2$ compositions.

(Some figures in this article are in colour only in the electronic version)

1. Introduction

The lead fluoride (β-PbF_2) and the lead–cadmium fluoride solid solutions ($Cd_{1-x}Pb_xF_2$) are representative of a class of fast ionic conductors with a fluorite structure in which the anions become highly mobile below the melting temperature. Ionic conductivities between 10^{-3} and 10^{-4} S cm^{-1} at 400 K have been reported for the solid solution with composition $0.33 \leqslant x \leqslant 0.7$, which are higher than those exhibit by CdF_2 ($\sigma \sim 10^{-7}$ S cm^{-1} at 400 K) and β-PbF_2 ($\sigma \sim 3 \times 10^{-5}$ S cm^{-1} at 400 K) [1, 17, 6, 22, 21]. These *superionic* solid solutions have attracted considerable attention because of their potential applications in solid-state batteries [18, 6, 5, 10].

[4] Author to whom any correspondence should be addressed.

Recent computational and experimental studies on the structural properties of lead–cadmium fluoride solid solutions, $Cd_xPb_{1-x}F_2$, have revealed intriguing details regarding its structural homogeneity [14, 12]. In general, the main experimental tool to observe the homogeneities of a system is x-ray diffraction and the observation that the lattice parameter follows Vegard's law. For the $Cd_xPb_{1-x}F_2$ systems, several experimental measurements [17] indicate that this system forms a homogeneous solid solution. However, Ohoro and White [11], have observed that an exsolution could occur on slow cooling, in agreement with other modeling [12, 14].

The melting curve of $Cd_xPb_{1-x}F_2$ systems as a function of Cd concentration has been measured by several authors [11, 8, 20, 15, 23]. All of them observed the same

phase diagram profile in which the melting curve presents a minimum around $x = 0.35$. Experiments by Ohoro and White [11] showed the minimum melting point at $T = 993$ K and $x = 0.40$. A slightly different result has been reported by Kozak [8] with $T = 1018$ K and $x = 0.30$. Sorokin *et al* [20] found a minimum at $T = 1023$ K and $x = 0.33$. More recent papers [15, 23] show $T = 1023$ K and $x = 0.35$, and $T = 1023$ K and $x = 0.33$, respectively. Molecular dynamic studies confirmed the minimum in the melt temperature at $x = 0.35$ [14, 12]. In this paper, we describe the CdF_2–PbF_2 solid solutions as a system that includes defects and a phase separation tendency, where the values of melting temperatures are more realistic and can serve as a source of new physical information to aid an understanding of the experiments.

These systems also present a fluorine-ion mobility attaining a superionic regime. Changes in the composition of this system considerably alter the superionic transition temperature. Several studies have been carried out to understand the dependence of fluorine-ion mobility [9, 25, 7, 24] as a function of composition. The maximum conductivity was first reported by Murin and Chernov [9]. Valakh *et al* [25] presented results from experimental and theoretical studies of the conductivity of $Cd_xPb_{1-x}F_2$ crystals at high temperature around the superionic region. When describing the experimental results of the dependence of the conductivity with composition, they found the maximum mobility for $x = 0.50$. Several other studies have being reported by Kosacki [7, 6] and Trnovcová [23] and all of them agree that the maximum conductivity occurs for $x = 0.33$. A very good list of related references can be found in Buchinskaya and Fedorov [2].

In this paper we will show that the maximum mobility for a given region of concentration is closely related to the inhomogeneity of the system in addition to its structural disorder.

Despite all the experimental effort which has being reported, it is still not clear under which condition $Cd_xPb_{1-x}F_2$ is a homogeneous or inhomogeneous system. In this paper we present molecular dynamics (MD) results which can clarify this lack of information. The main features of the model are the description of the clustering effect or nonrandom distribution of cations on a microscopic scale. Molecular dynamics simulation may help us to determine the role played by the cationic sublattice in the system homogeneity. In order to determine the loss of system homogeneity three procedures have been simulated using the MD simulation. The first process is an isothermal simulation of an undercooled liquid, the second is a solid obtained from slow cooling from the melt and the third one is the heating of the homogeneous glass, leading to its devitrification. From MD it is possible to quantify the inhomogeneity of the systems in these three processes.

2. Model and simulation procedures

The interaction potential for $Cd_xPb_{1-x}F_2$ systems is the two-body Buckingham potential given by:

$$V(r) = \frac{Z_i Z_j}{4\pi\varepsilon_0 r} + A_{ij}\exp(-r/\rho_{ij}) - \frac{C_{ij}}{r^6}.$$

Table 1. Values of parameters of Buckingham potential.

Atom pair	A (eV)	ρ (Å)	C (eV Å^6)
Pb–Pb	0	0	0
Cd–Cd	0	0	0
Pb–Cd	0	0	0
Pb–F	122.7	0.516	0
Cd–F	246.5	0.411	0
F–F	10 225	0.225	107.3

The values of the interatomic parameters were taken from previous simulations of PbF_2 [26] and CdF_2 [14]. The same set of interatomic potential parameters was used in the simulation for all compositions. The values of the parameters used in these simulations are listed in table 1. This interaction potential was recently used in molecular dynamics simulation of homogeneous solid solution [14, 12], and could correctly describe the minimum melting temperature at around $x = 0.35$.

The simulations were conducted in the NPT ensemble, with 2596 and 12 000 particles, at experimental density, and a periodic boundary condition was applied in order to avoid surface effects. All simulations were performed with the DL_POLY package [19].

Cooling and heating simulation processes were performed in $Cd_xPb_{1-x}F_2$ systems to evaluate the glass formation and devitrification features. The simulations start with an initial solid solution (ISS), an idealized system where lead atoms in the PbF_2 were randomly substituted by cadmium atoms at the desired concentration. From this ISS a liquid at 3000 K was obtained from where crystalline and amorphous phases were generated, using different cooling rates, at fixed pressure. Several cooling/heating rates were used: ultra-fast $q = 25$ K ps^{-1} (50 K each 2000 steps), fast $q = 1$ K ps^{-1} (10 K each 10 000 steps), slow $q = 0.2$ K ps^{-1} (1 K each 5000 steps) and ultra-slow $q = 0.025$ K ps^{-1} (1 K each 40 000 steps).

3. Results

As proposed previously [12], the phase segregation in these systems seems to occur when the liquid state is maintained at temperatures below the melting point, i.e. when the system is in an undercooled liquid state. In order to verify this property, an isothermal simulation was performed in which the liquid at 3000 K was quickly cooled down ($q = -25$ K s^{-1}) to 800 K, a temperature below the melting point for all compositions. The homogeneous undercooled liquid was then thermalized at this temperature during a 3500 ps simulation run. In the present system, the tetrahedral fluoride sites, in the fluorite lattice, give rise to five distinct local fluorine environments $Q^{(n)}$, corresponding to fluorine surrounded by nPb and 4-nCd neighbors ($0 \leqslant n \leqslant 4$), respectively, which can be used as a probe in the average local composition. The phase separation tendency during the evolution of the isothermal heat treatment was monitored by the evaluation of the frequency of the $Q^{(n)}$ sites as a function of time.

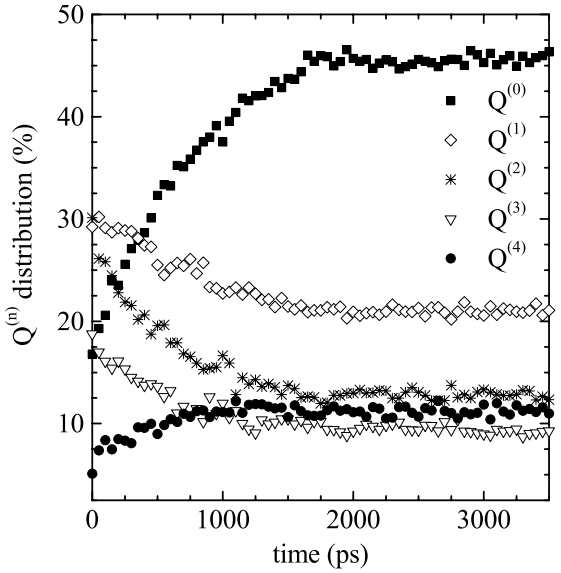

Figure 1. Time evolution of tetrahedral fluoride sites during the isothermal simulation of the undercooled liquid. System with 12 000 particles and $x = 0.50$ at $T = 800$ K. The loss of homogeneity in the Cd distribution is identified by the increase in the $Q^{(0)}$ tetrahedral fluoride sites in the first 2000 ps.

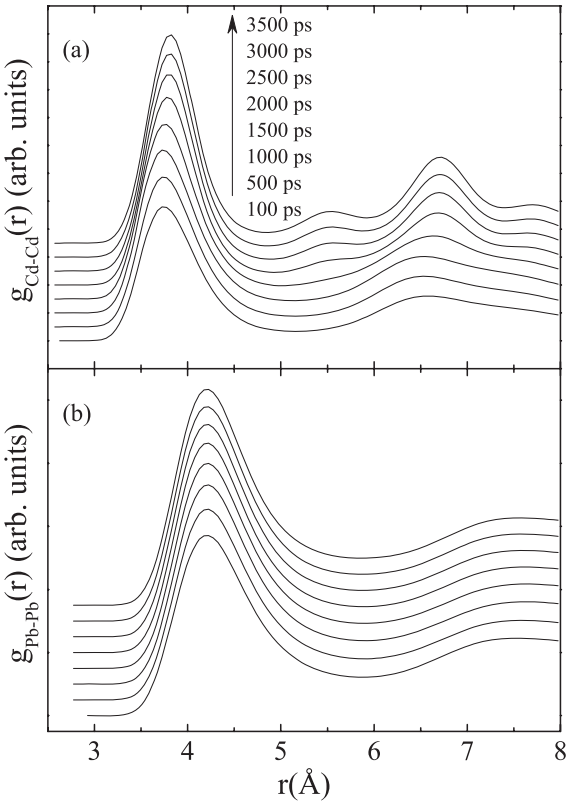

Figure 2. Partial pair distribution functions of the cationic sublattice of the system described in figure 1, calculated during a 3500 ps simulation run. After 2000 ps, time in which the phase separation takes place, the peaks in the $g_{\mathrm{Cd-Cd}}(r)$ indicate the crystallization of the Cd sublattice.

Figure 1 shows the evolution of the $Q^{(n)}$ sites during the isothermal simulation at $T = 800$ K, during 3.5×10^6 time steps (3500 ps) with $x = 0.5$ (the melting point for each concentration is shown in figure 6 and discussed below). The phase segregation tendency is reflected by the change in the distribution of $Q^{(n)}$ sites, mainly through the increase in the distribution of $Q^{(0)}$ and $Q^{(4)}$ sites, and the decrease of $Q^{(1)}$, $Q^{(2)}$ and $Q^{(3)}$ sites. Following the thermodynamic tendency of an undercooled melt, crystallization takes place after some time at this temperature, and this occurs after the phase separation process, as described below.

Figure 2 displays the evolution of the radial distribution functions for the Cd–Cd and Pb–Pb pairs, $g_{\mathrm{Cd-Cd}}(r)$ and $g_{\mathrm{Pb-Pb}}(r)$, respectively, with the progress of the isothermal simulation described above. The occurrence of well-defined peaks after 2000 ps, at the crystallographic interatomic distances, indicates that crystalline CdF_2-rich regions are formed before any PbF_2 crystallization takes place. Taking into account the evolution of the phase separation process shown in figure 1, one concludes that the phase separation precedes the crystallization.

As stated in our previous work [12] and evidenced here by the isothermal simulations described above, a phase separation tendency is observed while the liquid systems are maintained in an undercooled state. In order to avoid phase segregation, an ultra-fast cooling process (cooling rate of $q = -25$ K ps^{-1}) was performed from the liquid (3000 K) until the final temperature of 50 K was attained. The cooling of the liquid system at this rate gives rise to an homogeneous glasses (HG). This homogeneous glass was heated at a rate of $q = 0.025$ K ps^{-1}, and the devitrification properties analyzed.

Figure 3(a) depicts the volume per particle as a function of temperature for the processes discussed above. The composition with $x = 0.5$ is used as example. When the initial solid solution (ISS, black squares) is heated with a rate of $q = 0.2$ K ps^{-1}, the melting is observed at around 1330 K (not shown). The melting process of the other compositions was discussed in a previous paper [14], and led to a description of the phase diagram for the $Cd_xPb_{1-x}F_2$ system. An ultra-fast cooling of the homogeneous melt, with $q = -25$ K ps^{-1} (black triangles), gives origin to a frozen-in amorphous phase, with a higher volume per particle than the respective crystalline state. This amorphous solid is in a non-equilibrium thermodynamic state and can be considered as a glass, which devitrifies upon heating, in this case, at a rate $q = 0.025$ K ps^{-1} (circles). The glass transition temperature, T_g, can be obtained at the slope change in the cooling curve ($T_g \approx 450$ K) and the $Cd_{0.5}Pb_{0.5}F_2$ glass crystallization is observed upon heating at around 700 K, as expected, at a temperature above T_g. The devitrification process leads to a decrease in the volume, and minimizes the energy of the system leading to a stable, yet structurally imperfect, crystalline state, as indicated by the higher volume after devitrification, compared to the perfect, defect-free ISS. A snapshot of the crystallized glass at 800 K is depicted in figure 4 in three different orientations. The fluorine atoms are removed in order to better visualize the planes of crystallization and the inhomogeneities in the crystal. The melting of the devitrified system is attained at a lower temperature than the ISS, i.e. around 1110 K (not

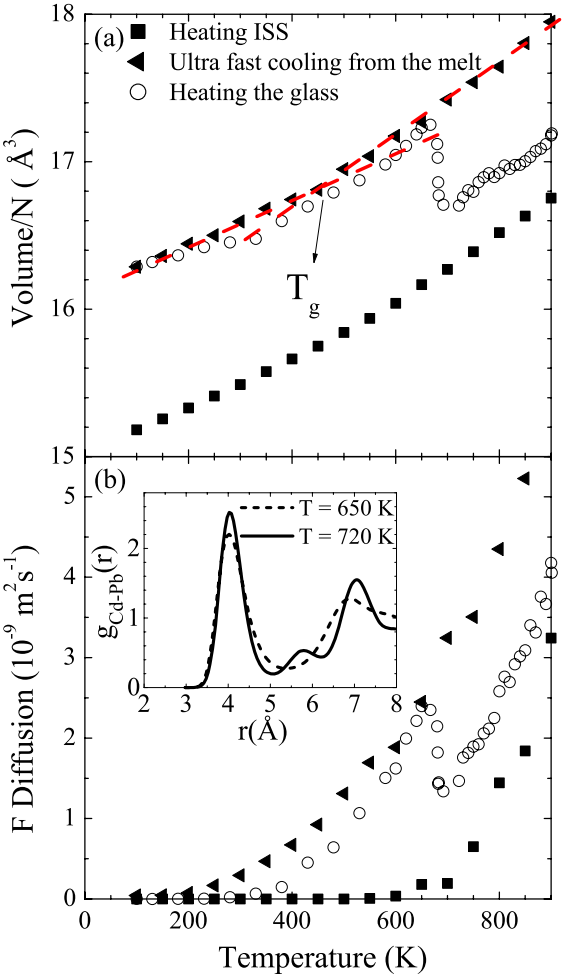

Figure 3. Volume per particle (a) and fluorine diffusion coefficient (b) as a function of temperature, of a system with $x = 0.50$ and 2592 particles, during the heating of the initial solid solution (squares), ultra-fast cooling from the melt (triangles) and heating of the obtained glass (open circles). The inset shows the Cd–Pb pair distribution function before (dotted line) and after crystallization (solid line).

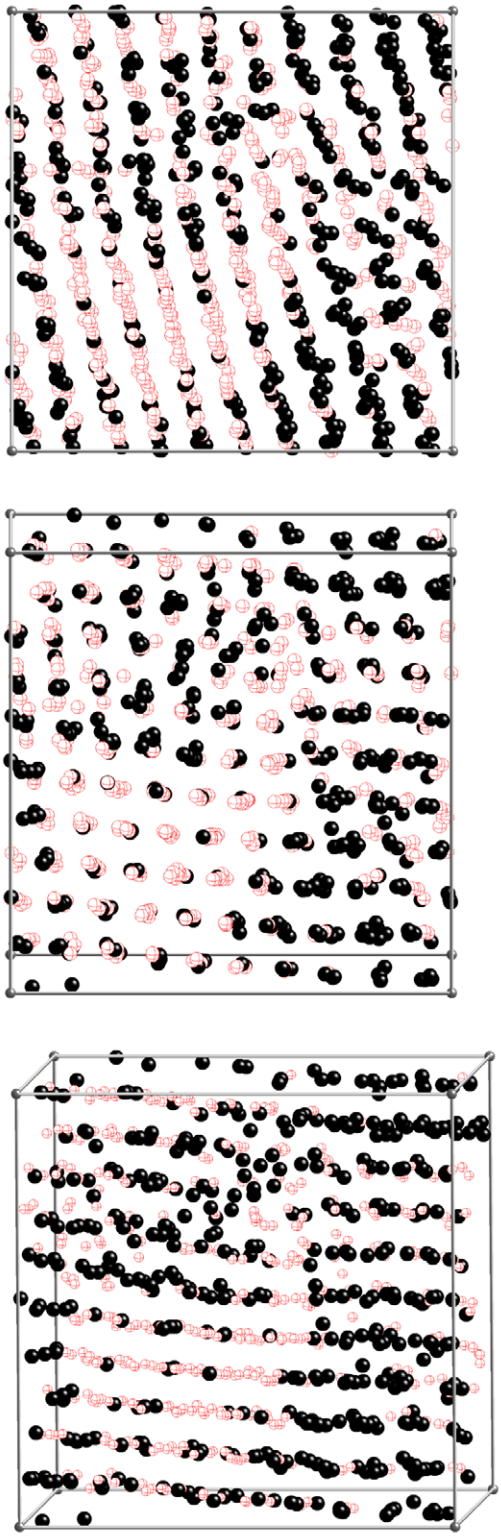

Figure 4. Snapshots for three different views of crystallized glass at 800 K and $x = 0.5$. These snapshots emphasize the crystalline planes and phase separation. Open spheres are the cadmium atoms, closed spheres are the lead atoms, and the fluorine atoms were left out in order to facilitate the visualization.

shown), mainly due to the structural defects in the crystalline state generated from the glass devitrification.

The fluorine diffusion coefficient, D_F, is an important probe to predict and explain the main ionic conduction features of these systems. Figure 3(b) shows the evolution of D_F as a function of the temperature, as the $Cd_{0.5}Pb_{0.5}F_2$ glass is heated. This figure clearly indicates that the fluorine diffusion process is greatly improved by the amorphous character of the diffusion sites, giving rise to a larger diffusion coefficient in the glass (triangles) than in the crystalline, defect-free, ISS (squares). This effect is in total accordance with previous studies, in which it was found that the anionic conductivity in glasses containing CdF_2–PbF_2 is larger than in the corresponding glass-ceramics [4].

The devitrification process, indicated by the step volume decrease during glass heating, as shown in figure 3(a), is confirmed through $g_{Cd-Pb}(r)$ inspection for the glass and crystallized systems, as shown in the inset of figure 3(b). The occurrence of well-defined peaks, related to the crystalline environment on the cationic arrangement, confirms the phase transformation from an amorphous structure, at 650 K, to a crystalline lattice, at 720 K. The fluorine diffusion coefficient

Table 2. Distribution of the occurrence of tetrahedral fluoride sites for all systems at $T = 50$ K.

x		$Q^{(0)}$	$Q^{(1)}$	$Q^{(2)}$	$Q^{(3)}$	$Q^{(4)}$
0.1	Statistical distribution	0.01	0.4	4.7	29.2	65.6
	ISS	0.12	0.58	5.67	26.74	66.90
	CG	0.06	0.65	4.64	27.60	67.04
	CM	0.35	1.71	6.19	20.24	71.50
0.2	Statistical distribution	0.2	2.6	15.4	41.0	41.0
	ISS	0.17	3.30	15.22	39.06	42.25
	CG	1.93	5.92	13.50	30.65	48.01
	CM	9.12	10.27	10.80	19.18	50.63
0.3	Statistical distribution	0.8	7.6	26.5	41.2	24.0
	ISS	0.75	7.99	26.85	39.70	24.71
	CG	16.27	10.13	8.56	12.55	52.48
	CM	11.76	8.44	9.06	17.98	52.77
0.4	Statistical distribution	2.6	15.4	34.6	34.6	13.0
	ISS	2.43	16.38	32.81	35.71	12.67
	CG	22.66	13.16	10.54	14.34	39.29
	CM	20.07	16.31	13.49	17.45	32.68
0.5	Statistical distribution	6.3	25	37.5	25	6.3
	ISS	6.02	25.58	37.38	24.42	6.60
	CG	20.34	21.67	18.89	17.75	21.35
	CM	20.07	16.31	13.49	17.45	32.68
0.6	Statistical distribution	13.0	34.6	34.6	15.4	2.6
	ISS	12.04	35.76	34.61	15.63	1.97
	CG	24.02	31.02	24.54	15.31	5.10
	CM	45.66	19.90	12.92	9.65	11.88
0.7	Statistical distribution	24.0	41.2	26.5	7.6	0.8
	ISS	23.09	42.82	25.93	7.41	0.75
	CG	37.42	32.85	18.34	8.94	2.45
	CM	52.70	24.10	11.60	7.24	4.37
0.8	Statistical distribution	41.0	41.0	15.4	2.6	0.2
	ISS	41.32	40.74	15.05	2.78	0.12
	CG	52.16	30.92	11.21	4.43	1.29
	CM	62.30	23.65	10.22	2.73	1.09

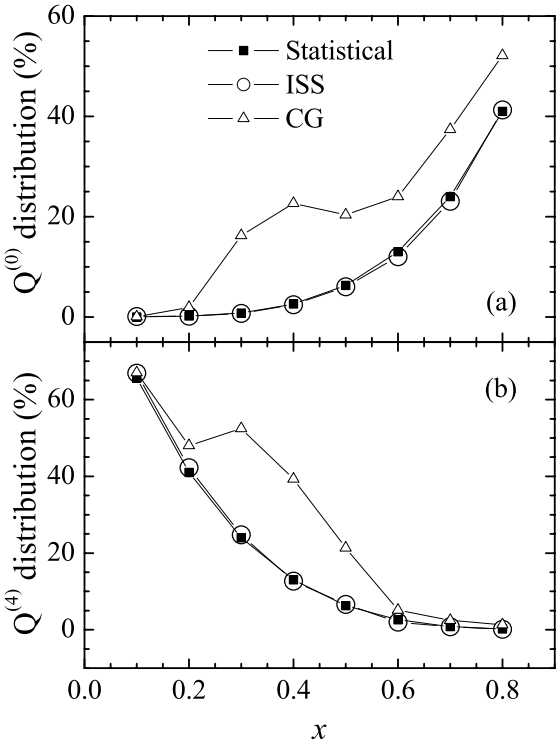

Figure 5. Tetrahedral fluoride sites $Q^{(0)}$ (a) and $Q^{(4)}$ (b), as a function of composition x for the calculated statistical distribution (squares), homogeneous (ISS, circles) and non-homogeneous (CG, triangles) crystalline systems at $T = 100$ K. The intermediate compositions of the CG systems present an expressive overestimation in the $Q^{(0)}$ and $Q^{(4)}$ sites in relation to the ISS system and statistical distribution.

decreases after the glass crystallization (circles), as the number of sites for the fluorine jump motion is restricted to the ones supplied by the crystalline system, in contrast to the unlimited paths observed in the amorphous structure of the glass.

However, as occurred in the case of the melt crystallization through slow cooling from the melt [12] or isothermal crystallization (figures 1 and 2), a PbF_2–CdF_2 phase separation precedes the devitrification process. Table 2 relates the $Q^{(n)}$ sites distribution for the studied compositions in the perfectly structurally organized initial solid solution (ISS), in the system slowly crystallized from the melt (CM), in the crystallized glass (CG), and in the calculated statistical distribution. The $Q^{(n)}$ distribution is clearly non-homogeneous in the CM and CG systems, and this particular arrangement was experimentally confirmed, in our previous work [12], by ^{19}F-NMR measurements.

Figure 5 shows, for sake of clarity, a plot of the data presented in table 2 of the percentage of $Q^{(0)}$ and $Q^{(4)}$ as a function of concentration. As noted above, the $Q^{(0)}$ and $Q^{(4)}$ sites correspond to $[FCd_4]$ and $[FPb_4]$, respectively, which can be considered as CdF_2 and PbF_2 clustering, i.e. phase separation. While an expected statistical distribution of $Q^{(0)}$ and $Q^{(4)}$ sites is observed in the defect-free ISS, an expressive deviation is observed for the system crystallized from the glass, with a maximum around the compositions with $x = 0.3$–0.4.

It is worth noting that, in our simulations, despite the fact that this phase segregation is observed in the $x = 0.2$–0.8 composition range, the cationic diffusion coefficients, D_{Cd} and D_{Pb}, indicate that, depending on the way the phase-separated crystalline state was produced (CM or CG systems), either a congruent or an incongruent melting process occurs. Figure 6 shows the evolution of the diffusion coefficient for the Cd and Pb atoms during the heating process of the CM and CG systems with $x = 0.35$ and 0.60. The melting transition is characterized by the step increase of the diffusion coefficient of the cationic species, reflecting the melting of the cationic lattice. For the CM system it was observed that phase segregation plays a major role in the melting process only in compositions with cadmium concentrations higher than 40 mol%, when the cadmium- and lead-rich phases melt separately. For compositions with $x \leqslant 0.35$ congruent melting is observed. As the system with $x = 0.35$ is the one with the minimum melting temperature on the entire composition range, the term 'eutectic composition' can be unambiguously employed [3, 13]. On the other hand, for the CG system, the congruent melting process is observed in the whole composition range. In figure 6, only compositions with $x = 0.35$ and 0.60 were shown, for the sake of simplicity, but all compositions on the CG system present a simultaneous step increase of the diffusion coefficient of the cationic species with temperature.

Besides the congruent melting process proposed above, the phase segregation trend during the crystalline solid solution

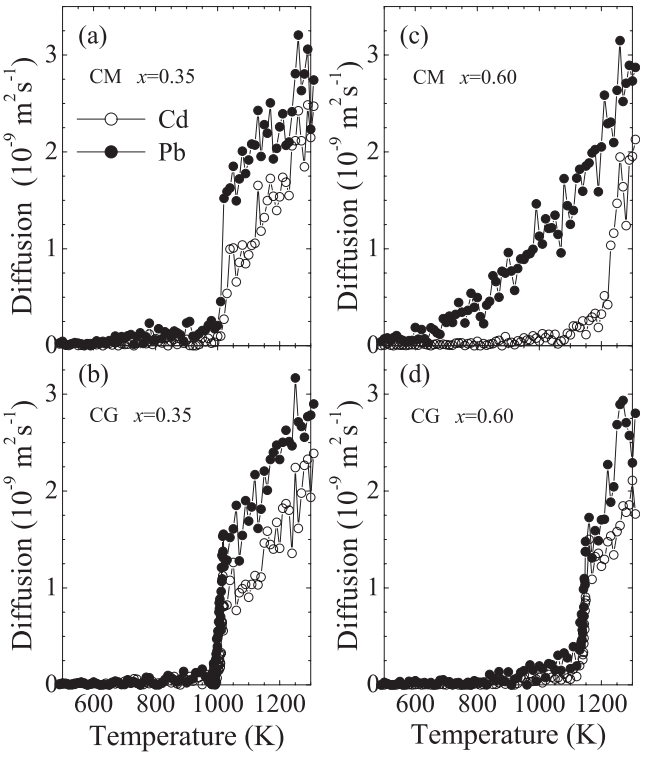

Figure 6. Cadmium (open circles) and lead (black circles) diffusion coefficients as a function of temperature for two compositions ($x = 0.35$ and 0.60) of the CM system ((a) and (b), respectively) and of the CG system ((c) and (d), respectively). The former presents an incongruent melting process for compositions with high Cd concentrations and the latter presents a congruent melting process for the whole composition range.

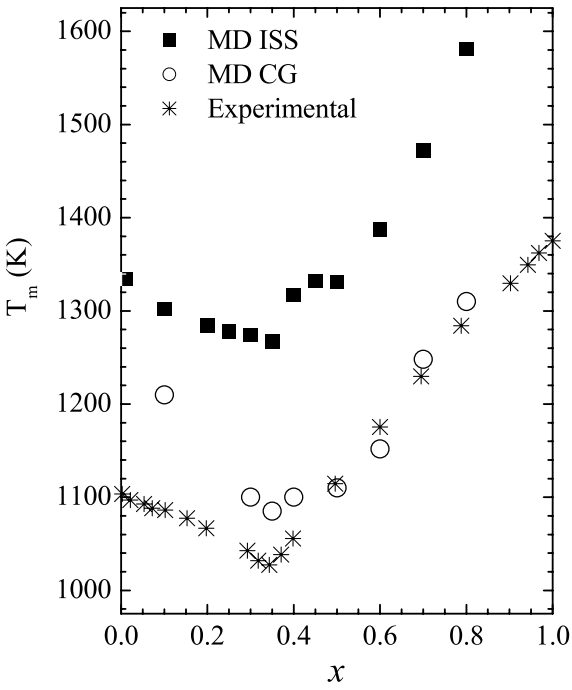

Figure 7. Melting temperature as a function of composition for the ISS (squares) and CG (circles) systems heated with $q = 0.2$ K ps^{-1}, compared with experimental data from Podsiadlo [15] (stars). All curves show a minimum around $x = 0.35$. The CG system properties permit a more realistic description of melting temperature.

formation is crucial to the development of a quantitative description of the melting and anionic conductivity processes on real systems, as described below.

Figure 7 shows the solid–liquid phase diagram, as obtained from the melting temperatures, T_m, of the defect-free ISS and those from the devitrified systems (CG), in the entire $Cd_xPb_{1-x}F_2$ composition range. For comparison purposes, the experimental data obtained from Podsiadlo [15] is also indicated. It is clear that the defects generated in the crystalline lattice during the glass devitrification is responsible for a decrease in the melting temperature and, differently from the perfectly crystalline ISS, a reasonable quantitative agreement in the solid–liquid phase diagram is observed between experimental and MD values.

The anionic conductivity of these systems, activated by the fluorine motions through the cationic lattice, is also directly affected by this kind of structural inhomogeneity, proposed by our simulation model. Figure 8 shows a plot of the ionic to superionic phase transition temperature as a function of the composition, x. The transition temperature values were arbitrarily defined as the temperature at which the fluorine diffusion coefficient attained the value 1×10^{-9} m^2 s^{-1}. These values were obtained during the heating process of the initial solid solution (ISS), the crystallized glass (CG), the crystalline material obtained from the cooling of the melt (CM) and the homogeneous glass (HG). The heating process of the crystalline systems ISS, CG and CM were performed at a rate of $q = 0.2$ K ps^{-1} and for the HG a rate of $q = 1$ K ps^{-1} was used, in order to avoid the glass crystallization during the diffusion coefficient measurements. Nevertheless, it is important to note that the fluorine diffusion values were observed as being independent of the heating rate. Figure 8 shows that the fluorine diffusion process, in the structurally perfect ISS, follows a linear dependence with composition, with an increase in the transition temperature value with cadmium content. A similar dependence of the diffusion coefficient with composition is observed for the homogeneous glass (HG) but, in this case, the transition temperature values are lower than those observed for the crystalline system. The amorphous nature of the vitreous state is the responsible for this decrease in the transition temperature, due to the large distribution of sites available for the ionic motion. On the other hand, for both crystallized systems, from the glass and from the melt (CG and CM, respectively), an inverse cupola is observed with a minimum at around $x = 0.3$, as reported experimentally [6, 7]. In this case, the dependence of the ionic to superionic transition temperature with composition attain values intermediate between the ones observed for the homogeneous crystalline (ISS) and glassy (HG) systems. Moreover, both crystallized systems (CG and CM) present CdF_2 and PbF_2 phase-segregated regions (see figure 4 for CG systems), and these results indicate that this phase separation trend is crucial in the correct reproduction of the conductivity properties on this kind of material.

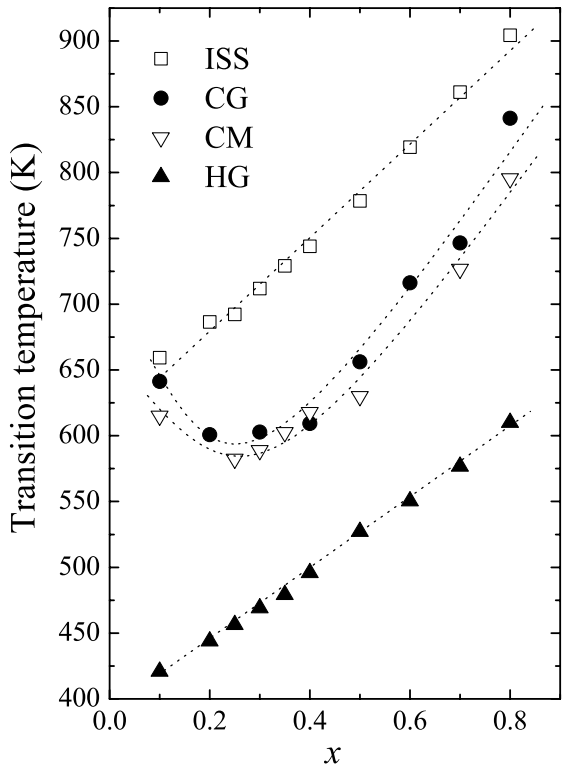

Figure 8. Ionic to superionic transition temperatures of the ISS (squares), CG (circles), CM (open down triangles) and HG (black up triangles) systems as a function of composition. The systems presenting phase separation (CG and CM) exhibit a minimum around $x = 0.35$, as expected experimentally, while the systems with a homogeneous distribution of cations exhibit a linear behavior.

4. Discussion

With the results presented above, we will discuss the importance of the inclusion of the phase segregation tendency in the description of the melting and fluorine diffusion processes of these systems. Obviously, this phase segregation must be interpreted, in real systems, as nano-sized Pb- (or Cd-) rich regions, dispersed through the crystalline matrix. In fact, other studies, including x-ray diffraction (XRD) and x-ray absorption spectroscopy (EXAFS) measurements have indicated homogeneous solid solution formation through the entire composition range when the mixed crystals were obtained by cooling of the melt [18]. On the other hand, Ohoro and White [11] have found the necessity of rapid cooling of $Cd_xPb_{1-x}F_2$ melts to not give rise to an exsolution. These findings indicate that the phase separation tendencies had already attracted the attention of researchers many years ago. Also, it is well known that CLAP glasses, i.e. glassy CdF_2–LiF–AlF_3–PbF_2 systems, present CdF_2 and PbF_2 segregation in the bulk material, during cooling of the melt and heating of the glass processes [16]. Our previous work [12], dealing with molecular dynamics simulations and ^{19}F NMR experiments, has also pointed out the direction of a β-PbF_2 phase segregation tendency.

Our results indicate that the phase separation takes place in the undercooled liquid state. In fact, a phase segregation process is clearly observed during the isothermal treatment at a temperature below the melting temperature, as represented by the evolution in time of $Q^{(n)}$ sites concentration, shown in figure 1. The increase of the concentration of $Q^{(0)}$ and $Q^{(4)}$ sites, and the decrease of $Q^{(1)}$, $Q^{(2)}$ and $Q^{(3)}$ sites clearly indicate the occurrence of CdF_2 and PbF_2 rich regions, and this feature is observed for all compositions $0.2 \leqslant x \leqslant 0.8$. During this isothermal treatment, the crystallization of the CdF_2-rich regions is observed before PbF_2, as shown in figure 2, in accordance with the higher melting point of the cadmium fluoride (m.p. $CdF_2 = 1076\,^{\circ}C$, m.p. $PbF_2 = 824\,^{\circ}C$) [15].

As depicted in figure 3(b), the amorphous nature of the glassy state favors the fluorine anion mobility, being the anionic diffusion coefficient of the glass larger than the one in the crystalline system. This is in total agreement with the jump model for the anionic conduction, in which the fluorine ions move over specific sites in the crystalline matrix, and that these preferred sites disappear in the amorphous broadening of sites distribution in the glass. In fact, the higher fluorine disordering around the lead atoms is reported to be the responsible for the better ionic conduction property of the composition with $x = 0.35$ [6, 18]. Our simulation results on the ISS (perfectly crystalline system) and HG (homogeneous glass) indicate (figure 8) that the ionic to superionic phase transition temperature is indeed favored by the amorphous nature of the glassy structure, compared to the crystalline structure of ISS. However its linear dependence with composition, observed in figure 8, disagrees with the experimental findings, as a nonlinear dependence of the evolution of the ionic conductivity with composition was reported [6, 7]. In this case, the results of the simulation of the ISS and HG systems simply reflects the fact that, in the interatomic potential proposed (table 1), the fluorine ions are more weakly attracted by the lead atoms than by the cadmium atoms, leading to a scheme where a fluorine atom close to a lead atom is more mobile than one close to a cadmium atom. The increase in the ionic–superionic temperature with the cadmium content simply reflects the higher concentration of F–Cd interactions.

Following the tendency of phase separation in the undercooled liquid state (figure 1), the crystallized system from slow cooling from the melt (CM) also presents CdF_2 and PbF_2 phase separation, as attested by the $Q^{(n)}$ sites survey shown in table 2. But this trend was also observed even in the homogeneous glass devitrification (CG), when a phase separation precedes the crystallization process (see figure 5). The diffusion coefficients of the cationic species, observed in figure 6, attest that a congruent melting process is observed for the crystallized glass, while an incongruent melt is observed for the system crystallized from the melt. We attribute this behavior to the fact that when the phase separation takes place in the undercooled melt (e.g., at 800 K), the higher mobility of the particles (low viscosity), due to the liquid state of the system, associated with the higher entropy of the system (high temperature), leads to a more efficient phase separation in the CM system. On the other hand, in the glassy state (or, at least, in the undercooled liquid just above T_g) the high viscosity of the system restricts the path lengths of the particle movements before devitrification, which leads to a less efficient phase

separation process in the CG system. Because the phase separation in the CG of all concentrations is less efficient, congruent melting occurs, as observed in figures 6 and 7, in contrast to the CM, which presents congruent melting only for compositions with $x \leqslant 0.35$.

We would like to emphasize that the phase separation tendency observed by our simulation model must be considered as an important issue in the complete understanding of the $Cd_xPb_{1-x}F_2$ solid solution properties, mainly considering the results shown in figures 7 and 8. From figure 6, it is clear that the profile of the solid–liquid phase diagram of these systems is independent of the occurrence of phase separation: the composition at which the melting temperature is minimum is correctly reproduced as being the one with $x = 0.35$. The absence of defects in the crystalline structure of the ISS leads to an overestimation of the melting temperatures, being approximately 200 K higher than those observed experimentally. The increase in the internal disorder in the range $0.1 \leqslant x \leqslant 0.35$, and a decrease in the range $0.35 \leqslant x \leqslant 0.9$ was previously attributed to be responsible for the occurrence of the minimum of the melting temperature for $x = 0.35$ [12]. The difference between experiment and theory disappears when the melting temperatures of the devitrified systems (CG) are computed, and the accordance with experimental data is very good. Once again, the occurrence of defects in the crystalline structure of the devitrified glass is the responsible for the decrease in the melting temperature, compared to the ISS. On the other hand, figure 8 points out the importance of the phase separation tendency on the ionic conduction properties of these materials. While the homogeneous (without phase separation) crystalline (ISS) and glassy (HG) systems present a linear dependence of the ionic–superionic transition temperature with concentration, the crystallized systems CM and CG, with the different phase separation degrees discussed above, present the experimentally expected inverse cupola, with the minimum transition temperature at around $x = 0.3$. This important result attests that phase segregation must be present in order to correctly reproduce the system's properties. Through this evidence we propose that the phase-segregated regions act as a conducting channel to the fluorine motions. In this context, figure 5 shows clearly that compositions near $x = 0.35$ present larger content of $Q^{(0)}$ and $Q^{(4)}$ sites in the CG system, compared to the statistical distribution and ISS, indicating the presence of $[FCd_4]$ and $[FPb_4]$ units, respectively. The increase in the structural inhomogeneity around the composition with $x = 0.35$ implies a better fluorine conducting property, in addition to a quantitatively good determination of the melting temperature of the $Cd_xPb_{1-x}F_2$ solid solutions.

5. Conclusion

We performed MD simulations in a NPT ensemble in order to study the structural properties of $Cd_xPb_{1-x}F_2$ solid solutions, during their formation from cooling from the melt and glass crystallization. The atomic configurations obtained presented some residual defects with a more or less expressive non-homogeneous distribution of components depending on the formation process. In this paper we demonstrate the importance of the inclusion of the phase segregation tendency in the discussion of the melting and fluorine diffusion processes (and ionic conductivity) of these systems. The phase segregation tendency reported here, to be considered as nano-sized chemically perturbed regions, implies in the correct description, not only qualitatively but also quantitatively, the melting temperature as well as the ionic–superionic phase transition temperature as a function of Cd concentration.

Acknowledgments

The Authors would like to thank the financial assistance of CAPES, FAPESP, FAPEMIG and CNPq, Brazilian agencies of research support.

References

[1] Boyce J B and Huberman B A 1979 Superionic conductors—transitions, structures, dynamics *Phys. Rep.* **51** 189–265
[2] Buchinskaya I I and Fedorov P P 2004 Lead difluoride and systems involving it *Usp. Khim.* **73** 404–34
[3] Buchinskaya I I and Fedorov P P 2008 Comment on 'The eutectic composition on $Cd_xPb_{1-x}F_2$ phase diagram: a molecular-dynamics study' by Picinin A, Silva M A P, Rino J P, and Hai G Q *Europhys. Lett.* **83** 16001
[4] Bueno L A, Donoso J P, Magon C J, Kosacki I, Filho F A D, Tambelli C C, Messaddeq Y and Ribeiro S J L 2005 Conductivity and F-19 NMR in $PbGeO_3$–PbF_2–CdF_2 glasses and glass-ceramics *J. Non-Cryst. Solids* **351** 766–70
[5] Julien C and Nazri G 1994 *Solid State Batteries: Materials Design and Optimization* (Boston, MA: Kluwer Academic)
[6] Kosacki I 1989 Physical-properties and applications of $Cd_{1-x}Pb_xF_2$ superionic crystals *Appl. Phys.* A **49** 413–24
[7] Kosacki I, Litvinchuk A P, Tarasov J J and Valakh M Y 1989 Anion disordering and specific-heat of $Cd_{1-x}Pb_xF_2$ super-ionic crystals *J. Phys.: Condens. Matter* **1** 929–34
[8] Kozak A D, Samouel M and Chretien A 1971 Crystalline miscibility of calcium, strontium and lead fluorides in cadmium fluoride–double fluoride Cd_2BaF_6 *Rev. Chim. Miner.* **8** 805
[9] Murin I V and Chernov S V 1982 Electrical-properties of solid-solutions in the PbF_2–CdF_2 system *Inorg. Mater.* **18** 149–50
[10] Netshisaulu T T, Chadwick A V, Ngoepe P E and Catlow C R A 2005 Spectroscopic and computer modelling studies of mixed-cation superionic fluorites *J. Phys.: Condens. Matter* **17** 6575–86
[11] Ohoro M P and White W B 1971 Phase equilibria in systems CdF_2–CaF_2, CdF_2–PbF_2, and CdF_2–ZnF_2 *J. Am. Ceram. Soc.* **54** 588
[12] Picinin A, Deshpande R R, de Camargo A S S, Donoso J P, Rino J P, Eckert H and Silva M A P 2008 Structural ordering in $Cd_xPb_{1-x}F_2$ alloys: a combined molecular dynamics and solid state NMR study *J. Chem. Phys.* **128** 224705
[13] Picinin A, Silva M A P and Rino J P 2008 Reply to the comment by I I Buchinskaya and P P Fedorov *Europhys. Lett.* **83** 16002
[14] Picinin A, Silva M A P, Rino J P and Hai G Q 2005 The eutectic composition on CdxPb1-F-x(2) phase diagram: a molecular-dynamics study *Europhys. Lett.* **71** 770–5
[15] Podsiadlo H 1998 Phase equilibria in the binary system lead fluoride $[PbF_2]$–cadmium fluoride $[CdF_2]$ *J. Therm. Anal. Calorim.* **54** 863–6
[16] Randall M S, Simmons J H and Elbayoumi O H 1988 Primary and secondary phase-separation in CdF_2–LiF–AlF_3–PbF_2 glasses *J. Am. Ceram. Soc.* **71** 1134–41

[17] Samara G A 1979 Pressure and temperature dependences of the ionic conductivities of cubic and orthorhombic lead fluoride (PbF_2) *J. Phys. Chem. Solids* **40** 509–22

[18] Silva M A P, Messaddeq Y, Briois V, Poulain M, Villain F and Ribeiro S J L 2002 Structural studies on lead–cadmium fluoride solid solutions *Solid State Ion.* **147** 135–9

[19] Smyth W and Forester T R 1996 Dl Poly. pp DL_POLY is a packageof molecular-simulation routines written by Smyth W and Forester T R *Copyright The Council for the Central Laboratory of the Research Councils* Daresbury Laboratory, Nr Warrington

[20] Sorokin N I, Buchinskaya I I and Sobolev B P 1992 Ionic-conductivity of $Pb_{0.67}Cd_{0.33}F_2$ and $Pb_{0.67}Cd_{0.33}F_2Ce_3$ + monocrystals *Zh. Neorg. Khim.* **37** 2653–6

[21] Sorokin N I, Sobolev B P and Breiter M W 2002 Specific features of anion transfer in superionic conductors based on MF_2 (M = Pb and Cd) *Phys. Solid State* **44** 1579–86

[22] Trnovcova V, Fedorov P P, Buchinskaya I I, Smatko V and Hanic F 1999 Fast ionic conductivity of PbF_2:MF_2 (M = Mg, Ba, Cd) and PbF_2:ScF_3 single crystals and composites *Solid State Ion.* **119** 181–9

[23] Trnovcova V, Fedorov P P, Ozvoldova M, Buchinskaya I I and Zhurova E A 2003 Structural features of fluoride-ion transport in $Pb_{0.67}Cd_{0.33}F_2$ single crystals *J. Optoelectron. Adv. Mater.* **5** 627–34

[24] Valakh M Y, Kosacky I, Kushnir E Y, Litvinchuk A P and Tarasov G G 1988 Effect of entropic and energy factors on the phase-transition in the superionic semiconductors $Pb_xCd_{1-X}F_2$ *Fiz. Tverd. Tela* **30** 3467–70

[25] Valakh M Y, Kosatskii I, Litvinchuk A P and Tarasov G G 1985 Lattice-dynamics peculiarities and ionic-conductivity of mixed $Pb_xCd_{1-X}F_2$ superionic crystals *Fiz. Tverd. Tela* **27** 3667–71

[26] Walker A B, Dixon M and Gillan M J 1982 Computer-simulation of ionic disorder in high-temperature PbF_2 *J. Phys. C: Solid State Phys.* **15** 4061–73